Nonlinear modeling of thermoacoustic systems

J.A. de Jong, Y.H. Wijnant, A. de Boer
Department of Engineering Technology, University of Twente, Enschede, The Netherlands.

D. Wilcox
Chart Inc. - Qdrive, 302 Tenth St., Troy, NY 12180, USA

Abstract
Thermoacoustic systems convert energy from heat to acoustic power and vice versa. These systems have commercial interest due to the high potential efficiency and low number of moving parts. To numerically predict the performance of a thermoacoustic device inherent nonlinearities in the system, such as thermoacoustic streaming and generation of harmonics need to be taken into account. We present a nonlinear frequency domain method with which these nonlinearities in thermoacoustic systems are modeled in a computationally efficient manner. Using this method, the nonlinear periodic steady state of a thermoacoustic engine can directly be computed, without computing the long initial transient of the system. In this publication, the developed method is applied to compute the periodic steady state of an experimental standing wave engine. The results obtained match well with experimental data.

PACS no. 43.35.Ud,43.25.Ts,43.25.Gf

1. Introduction

Thermoacoustic (TA) systems utilize the physical interaction between heat and sound [1] to perform a thermodynamic cycle. The main advantage of the technology are the low number of moving parts and high reliability. For thermoacoustic Stirling systems, also the conversion efficiency between heat and sound can be high due to the use of the efficient Stirling cycle [2]. Two classes of operation can be distinguished: engines and refrigerators/heat pumps. In a TA engine heat is used to generate acoustic power, which can subsequently be used to generate electrical power. In a TA heat pump or refrigerator, acoustic power is used to pump heat between two thermal reservoirs from cold to hot.

In this paper, a nonlinear model for thermoacoustic devices is presented. The simulation time is significantly reduced by directly solving the periodic steady state of the system. This nonlinear model is able to describe nonlinear effects in TA systems [3], such as the generation of harmonics [4] and Gedeon streaming [5]. We will demonstrate the model by simulating a standing wave thermoacoustic engine [6] in its periodic steady state.

2. Model

2.1. One-dimensional equations

In TA systems the wave propagation is mostly one-dimensional. As a result, the pressure can be assumed to be constant in the plane transverse to the wave propagation direction, and the governing equations of fluid dynamics can be integrated along the transverse directions. This results in a set of one-dimensional equations which contain source terms describing the interaction of the fluid with the surrounding solid. Slowly varying changes in the cross-sectional area are accounted for. We assume ideal gas behavior so the specific heats of the fluid are constant and the gas obeys the perfect gas equation of state. Additionally, for simplicity we assume the dynamic viscosity (μ) and thermal conductivity (κ) are constant. A detailed derivation of the model is shown by Watanabe *et al.* [7] The area-averaged continuity equation is

$$\frac{\partial \rho}{\partial t} + \frac{1}{S_f}\frac{\partial}{\partial x}\left(S_f \rho u\right) = 0, \tag{1}$$

where x is the wave propagation direction, t is time, $\rho(x,t)$ is the area-averaged density, $S_f(x)$ the cross-sectional area occupied by fluid, and $u(x,t)$ the velocity in the wave propagation direction. The area-averaged momentum equation in the propagation direction is

$$\frac{\partial}{\partial t}\left(\rho u\right) + \frac{1}{S_f}\frac{\partial}{\partial x}\left(S_f \rho u^2\right) + \frac{\partial p}{\partial x} = -\mathcal{R}, \tag{2}$$

where $p(x,t)$ is the pressure and $\mathcal{R}$ is the resistive drag force (unit $\mathrm{N{\cdot}m^{-3}}$) in the wave propagation direction due to shear stress at the wall acting on the fluid. The pressure is assumed to be constant along the transverse direction. The area-averaged total energy equation is

$$\frac{\partial}{\partial t}\left(\frac{p}{\gamma-1}+\frac{1}{2}\rho u^2\right)+ \frac{1}{S_f}\frac{\partial}{\partial x}\left[uS_f\left(\frac{\gamma}{\gamma-1}p+\frac{1}{2}\rho u^2\right)-\kappa S_f\frac{\partial T}{\partial x}\right]= +\mathcal{H}-\mathcal{Q}\frac{dT_w}{dx}, \quad (3)$$

where $T(x,t)$ is the area-averaged fluid temperature, $T_w(x)$ is the temperature of the solid wall and γ the ratio of specific heats. The wall temperature is a prescribed function of the position. Together, $\mathcal{H}(\rho,T,T_w)$ and $\mathcal{Q}(\rho,T,u)$ model heat transfer from the wall to the fluid. The unit of $\mathcal{H}$ is $\mathrm{W{\cdot}m^{-3}}$. The terms $\mathcal{R}$, $\mathcal{Q}$, and $\mathcal{H}$ will be described in Sec. (2.3). The last equation in this set is the perfect gas equation of state

$$p=\rho R_s T, \quad (4)$$

where R_s is the specific gas constant.

2.2. Nonlinear frequency domain method

The time dependence of all variables is assumed to be periodic. Hence, all dependent variables $\xi=\rho,p,T,u$ can be described by a Fourier series:

$$\xi(x,t)=\Re\left[\sum_{n=0}^{\infty}\hat{\xi}_n(x)e^{in\omega t}\right], \quad (5)$$

where $i=\sqrt{-1}$, $\hat{\xi}_n$ are the complex-valued Fourier coefficients, ω the fundamental angular frequency and n the harmonic number. $\Re[\cdots]$ denotes the real part. Assuming a decaying spectrum, we can approximate the response by truncating the Fourier series up to N_f harmonics. Substituting this truncated Fourier series for $\xi=\rho,p,T,u$ in Eqs. (1-4) yields a nonlinear system of *ordinary* differential equations in x. These differential equations contain nonlinear terms in the form of products of the truncated Fourier series. Following the nonlinear frequency domain (NLFD method [8], these nonlinear terms are computed by first applying an inverse discrete Fourier transform to obtain time domain samples, then computing the nonlinear terms, and subsequently transforming back to the frequency domain.

The resulting system of equations is discretized in space using the finite volume method. The final nonlinear system of algebraic equations is solved using the Newton-Raphson method [9], using an exact evaluation of the Jacobian matrix. A detailed description of the implementation will be published elsewhere [10].

2.3. The exchange terms

The momentum and heat exchange terms with the solid, $\mathcal{R}$, $\mathcal{Q}$, and $\mathcal{H}$ are derived from linear thermoacoustic theory [11, 12]. This theory is defined in the frequency domain. Therefore, the resulting expressions can straightforwardly be used in the NLFD form of Eqs. (1-4). The closed form expression for the Fourier coefficients of the viscous resistance $\mathcal{R}$ are found to be [13]

$$\hat{\mathcal{R}}_n=\frac{\mu}{r_h^2}\frac{is_n^2 f_{\nu,n}}{1-f_{\nu,n}}\hat{u}_n, \quad (6)$$

where r_h is the hydraulic radius: the fluid cross sectional area divided by the the wetted perimeter of the geometry, s_n is the shear wave number [14] at harmonic n:

$$s_n=r_h\sqrt{\frac{\hat{\rho}_o\omega n}{\mu}}, \quad (7)$$

and $f_{\nu,n}(s_n)$ the cross-sectional geometry dependent viscous Rott function, evaluated at the shear wave number s_n. For example, for parallel plates this function is [1]:

$$f_{\nu,n}(s_n)=\frac{\tanh\left(\sqrt{i}\,s_n\right)}{\sqrt{i}\,s_n}. \quad (8)$$

Similar to the result for $\hat{\mathcal{R}}_n$, the Fourier coefficients of $\mathcal{H}$ and $\mathcal{Q}$ are

$$\hat{\mathcal{H}}_n=\frac{\mathrm{Pr}\,\kappa}{r_h^2}\frac{is_n^2 f_{\kappa,n}}{1-f_{\kappa,n}}, \quad (9)$$

$$\hat{\mathcal{Q}}_n=\frac{\hat{\rho}_0 c_p}{1-\mathrm{Pr}}\left(\frac{f_{\nu,n}}{1-f_{\nu,n}}-\mathrm{Pr}\,\frac{f_{\kappa,n}}{1-f_{\kappa,n}}\right), \quad (10)$$

where Pr is the Prandtl number, c_p the specific heat at constant pressure and $f_{\kappa,n}(s_n,\mathrm{Pr})$ the thermal Rott function evaluated for shear wave number s_n. The viscous and thermal Rott functions are related as:

$$f_{\kappa,n}(s_n,\mathrm{Pr})=f_{\nu,n}(\sqrt{\mathrm{Pr}}\,s_n). \quad (11)$$

3. Application: standing wave thermoacoustic engine

Figure (1) schematically shows the experimental standing wave thermoacoustic engine of Atchley [6]. It consists of 5 segments, the resonator, the cold heat exchanger (HX), the stack, the hot HX and the hot end. The dimensions of this engine are listed in Table (I). The total length is $L=0.98\,\mathrm{m}$. The cross sectional area of all segments in the engine is $1.14{\cdot}10^{-3}\,\mathrm{m}^2$. The fluid cross-sectional area S_f can be obtained by multiplying the tabulated porosity (ϕ) with this cross-sectional area. The resonator and hot end are modeled as circular tubes with a porosity of 1. The cold HX,

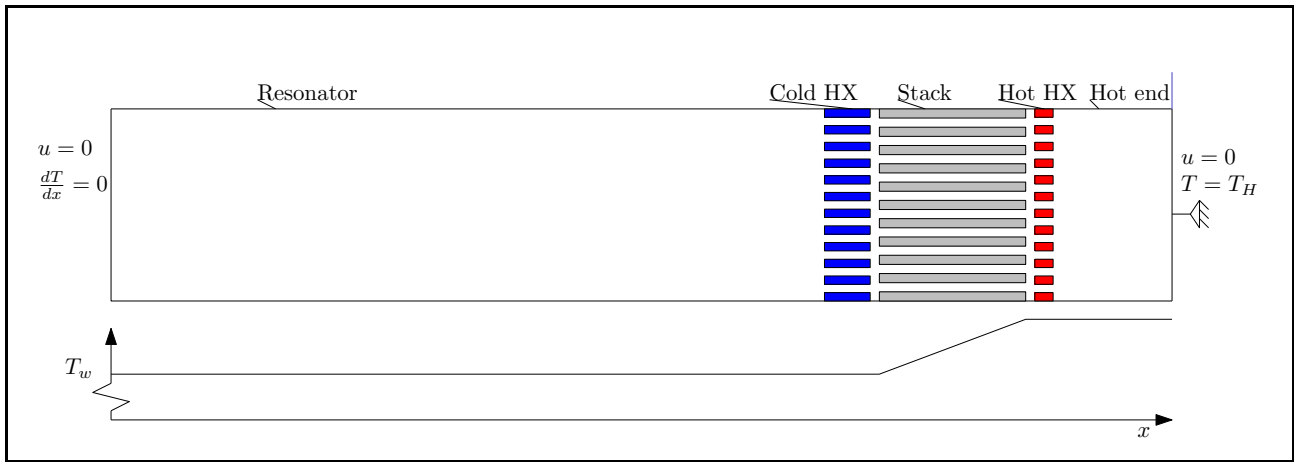

Figure 1. Schematic overview of the standing wave engine of Atchley [6]. The figure is not at scale. The prescribed wall temperature profile is shown in the graph below. At the right side of the stack, T_w is set to T_H. The boundary conditions on the left and right side are shown.

Table I. Geometrical data of the standing wave engine of Atchley.

Segment	Length (mm)	r_h (mm)	ϕ
Resonator	879.7	9.55	1.00
Cold HX	20.4	0.51	0.70
Stack	35.0	0.385	0.73
Hot HX	7.62	0.51	0.70
Hot end	473.0	9.55	1.00

stack and hot HX are modeled as parallel-plate segments with plate-to-plate spacing of $2r_h$.

The heat exchangers provide the heat to enable a temperature gradient across the stack. Due to this temperature gradient, acoustic power is generated in the stack. No mechanism is present to convert the generated acoustic power, hence all acoustic power is dissipated in the resonator and the hot end.

The cold HX temperature and resonator wall temperature is kept constant at $T_0 = 20\,^{\circ}\mathrm{C}$, whereas the hot HX and hot end wall temperature are kept at $T_H = T_0 + \Delta T$. At the left and right side of the segment the velocity is set to zero, in accordance with the no-slip boundary condition. The working gas is helium, at a mean pressure of $p_0 = 376\,\mathrm{kPa}$.

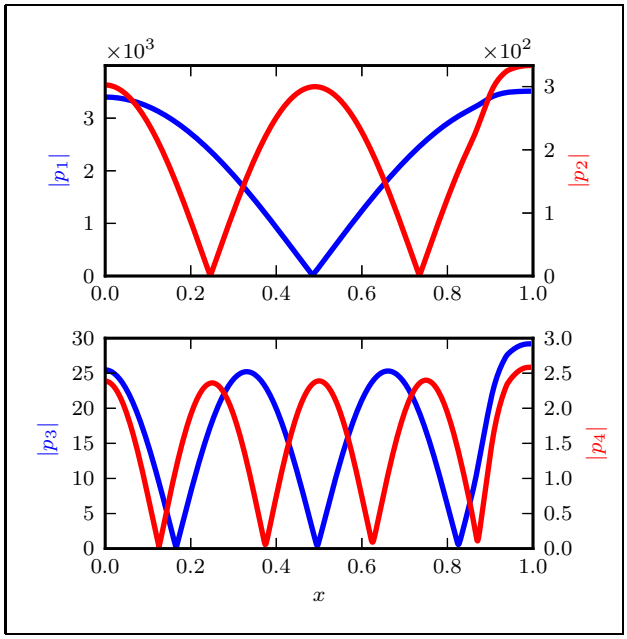

Figure 2. Absolute value of the first four pressure Fourier coefficients as a function of the position in the engine at $\Delta T = 325\,\mathrm{K}$.

4. Results

A convergence study showed that a total number of grid-points of 1059 and a number of harmonics of 6 is sufficient to make the results nearly independent of these parameters. The onset ΔT is the temperature difference at which the the pressure in the engine spontaneously starts oscillating. This temperature difference is found to be slightly below 325 K. At this temperature difference, the fundamental frequency is found to be 516 Hz, which is close to the eigenfrequency corresponding to the first acoustic eigenmode of an empty tube: $c_0/(2L) = 504\,\mathrm{Hz}$. Figure (2) shows the absolute value of the first four pressure harmonics as a function of the position at ΔT =325 K. The magnitudes of these amplitudes indicate a decaying spectrum. The first and second harmonic show nearly perfect nodes, indicating a high standing wave ratio. The increase in amplitude of p_2, p_3 and p_4 on the right side is due to the influence of the stack and heat exchangers.

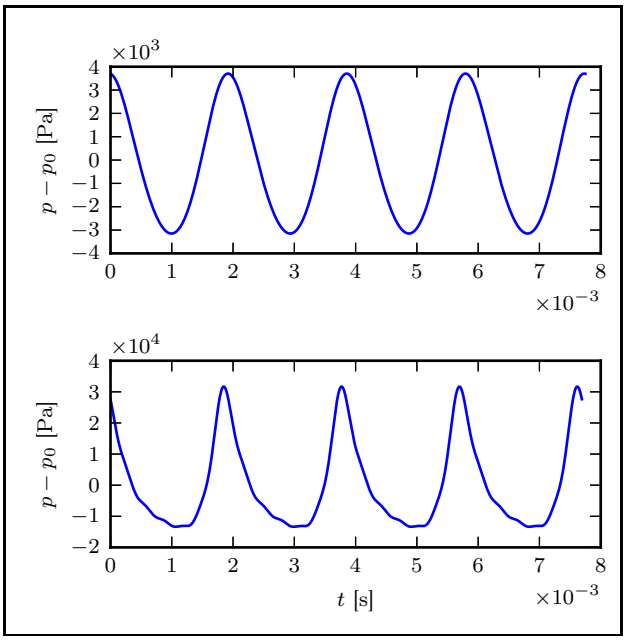

Figure 3. Computed time response of the pressure for different ΔT. Above: $\Delta T = 325\,\mathrm{K}$, below: $\Delta T = 365\,\mathrm{K}$. The mean pressure is subtracted.

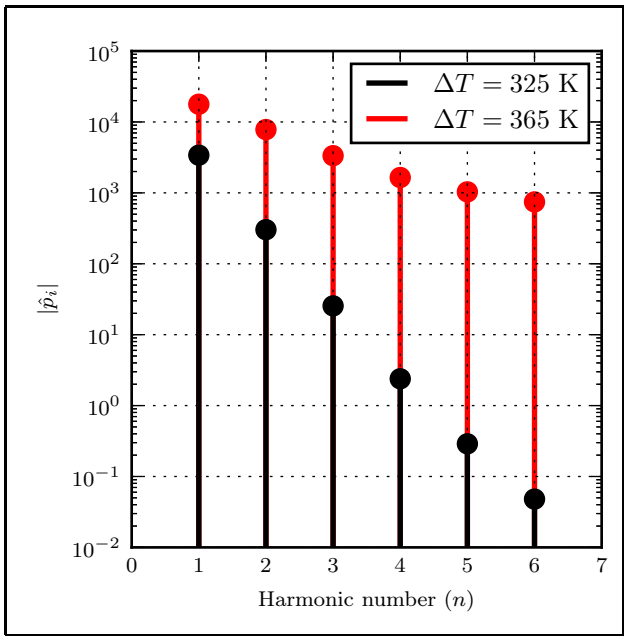

Figure 4. Spectrum of the two plots of Fig. (3).

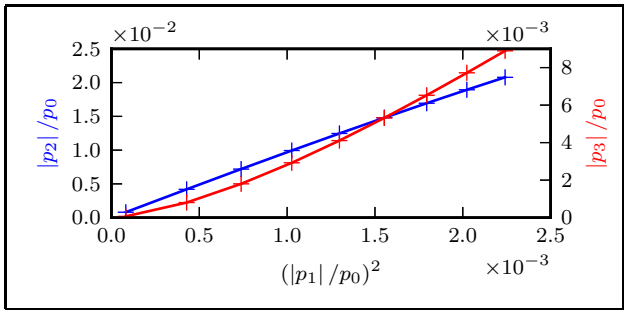

Figure 5. Scaled amplitude of p_2 and p_3 at $x = 0$ vs. the square of the scaled amplitude of the first harmonic at $x = 0$.

Temperature dependence

The response of the system is studied for different values of the controlling parameter ΔT. This temperature is increased in steps of 5 K from $\Delta T = 325\,^{\circ}\mathrm{C}$ to 365 °C. At $\Delta T = 325\,^{\circ}\mathrm{C}$, the computed amplitude of the first harmonic is $3.4{\cdot}10^3$ Pa, whereas at $\Delta T = 365\,^{\circ}\mathrm{C}$ the amplitude is nearly tripled to $1.8{\cdot}10^4$ Pa.

Figure (3) shows a time response of the pressure at the left side of the tube for the lowest (top) and highest (bottom) ΔT. Figure (4) shows the magnitude of the spectrum of Fig. (3). As is visible, the time response at the highest temperature is significantly distorted. This is a result of nonlinear effects, which redivide acoustic energy between the fundamental harmonic and the higher harmonics. This is also reflected in the spectrum, which shows less decay with increasing n. The time response of the pressure of Figure (3) shows good agreement with the experimental results of Atchley [15]. This validates the correct implementation of the numerical method.

Figure (5) shows the normalized amplitude of the second and third harmonic as a function of the square of the normalized amplitude of the first harmonic. These results indicate that the second harmonic is approximately proportional to $|p_1|^2$, which agrees with the experimental results obtained by Swift [3].

5. Conclusions

A standing wave thermoacoustic engine is simulated with a nonlinear model for thermoacoustic devices. With this model, nonlinear effects such as Gedeon streaming and the generation of harmonics in thermoacoustic systems can be modeled. The periodic steady-state is directly computed using the nonlinear frequency domain method. By omitting the computation of the long initial transient that follows the onset of the system, the computational cost is significantly reduced. This allows for the use of a nonlinear model for thermoacoustic system design optimization. The obtained results show good agreement with literature data, thereby validating the method and numerical implementation.

Further research will involve the use of this model for simulating thermoacoustic systems which are more commercially interesting, such as thermoacoustic Stirling heat engines and pulse tube cryocoolers.

Acknowledgement

This research has been carried out as a part of the Agentschap NL EOS-KTO (KTOT03009) research program. The financial support is gratefully acknowledged.

References

[1] G. W. Swift. *Thermoacoustics: A unifying perspective for some engines and refrigerators*. Melville, NY: Acoustical Society of America, 2003.

[2] S. Backhaus and G. W. Swift. "A thermoacoustic Stirling heat engine". *Nature* 399.6734 (27, 1999), pp. 335–338.

[3] G. W. Swift. "Analysis and performance of a large thermoacoustic engine". *The Journal of the Acoustical Society of America* 92.3 (1992), pp. 1551–1563.

[4] S. Karpov and A. Prosperetti. "Nonlinear saturation of the thermoacoustic instability". *The Journal of the Acoustical Society of America* 107.6 (2000), pp. 3130–3147.

[5] D. Gedeon. "DC gas flows in Stirling and pulse tube refrigerators". *Cryocoolers* 9 (1997), pp. 385–392.

[6] A. A. Atchley. "Study of a thermoacoustic prime mover below onset of self-oscillation". *The Journal of the Acoustical Society of America* 91 (1992), pp. 734–743.

[7] M. Watanabe, A. Prosperetti, and H. Yuan. "A simplified model for linear and nonlinear processes in thermoacoustic prime movers. Part I. Model and linear theory". *The Journal of the Acoustical Society of America* 102 (1997), pp. 3484–3496.

[8] K. C. Hall et al. "Harmonic balance methods applied to computational fluid dynamics problems". *International Journal of Computational Fluid Dynamics* 27.2 (2013), pp. 52–67.

[9] W. H. Press et al. *Numerical recipes in C*. 2nd ed. New York, NY, USA: Cambridge University Press, 1997.

[10] J. A. de Jong et al. "A frequency domain method for solving periodic nonlinear acoustic problems". *To be published* (2015).

[11] G. W. Swift. "Thermoacoustic Engines". *The Journal of the Acoustical Society of America* 84.4 (1988), pp. 1145–1180.

[12] N. Rott. "Damped and thermally driven acoustic oscillations in wide and narrow tubes". *Zeitschrift fÃŒr angewandte Mathematik und Physik* 20.2 (1969), pp. 230–243.

[13] J. A. de Jong et al. "Modeling of thermoacoustic systems using the nonlinear frequency domain method". *To be published* (2015).

[14] H. Tijdeman. "On the propagation of sound waves in cylindrical tubes". *Journal of Sound and Vibration* 39.1 (8, 1975), pp. 1–33.

[15] A. Atchley, H. Bass, and T. Hofler. "Development of Nonlinear Waves in a Thermoacoustic Prime Mover". *Frontiers of Nonlinear Acoustics*. 12th ISNA. Elsevier Science Publishers Ltd, London, 1990, pp. 603–608.